

# The Equation of State with EPOS model

Maria Stefaniak

*Warsaw University of Technology,  
pl. Politechniki 1, 00-661 Warsaw, Poland  
GSI Helmholtzzentrum für Schwerionenforschung,  
Planckstr. 1, 64291 Darmstadt, Germany*

Klaus Werner

Johannès Jahan

*SUBATECH, University of Nantes – IN2P3/CNRS – IMT Atlantique, Nantes, France*

Hanna Zbroszczyk

*Warsaw University of Technology, pl. Politechniki 1, 00-661 Warsaw, Poland*

(Dated: September 28, 2022)

Transitions between different states of matter and their thermodynamical properties are described by the Equation of State (EoS). A universal representation of the equation of state of QCD for the whole phase diagram has not yet been determined. Expectation of the systems to undergo various types of transitions depending on the temperature, the chemical potential  $\mu_B$  and other thermodynamical features makes that puzzle even more challenging to solve. Furthermore, it is not apparent which experimentally measurable observables could provide the useful information for the determination of EoS. The application of different EoS for hydrodynamical evolution was introduced in the EPOS generator, what allowed to study the effect of its changing on the final observables. The family of EoS proposed by the BEST Collaboration was implemented. The Critical Point position and the strength of criticality variations were investigated with particle yield, transverse momentum spectra, flow, and moments of the net-proton distributions.

## I. INTRODUCTION

The determination of the Equation of State (EoS) is crucial for the complete description and understanding the QCD phase diagram. The rules of physics have to be universal for all the systems existing in nature. The relations between thermodynamical quantities characterizing different states of nuclear matter are depicted in the construction of EoS. The substantial topic of present research is investigation of various transitions between partonic and hadronic medium. It is expected to undergo diverse processes depending on the temperature and baryon-chemical potential ( $\mu_B$ ) of the medium. EoS expresses the relations between various matter parameters such as pressure, temperature, energy density, speed of sound, and former. It is not trivial to characterise the whole phase diagram area. Consequently, such features of QCD as chiral symmetry breaking or confinement, are not fully understood. There are various attempts performed to generate the EoS, which will allow one to characterise the whole QCD phase diagram, starting from  $\mu_b = 0$  ending on cold neutron stars [1]. These EoS introduce the first-order phase transition for finite baryochemical potential and relatively lower temperatures. Nevertheless, some of them provide information about the Critical Point location and properties of this transition [2, 3].

## II. BEST EQUATION OF STATE

Collaboration Beam Energy Scan Theory (BEST) proposed a family of Equations of State describing the same region of QCD phase diagram as studied in the BES program [3, 4]. It covers the region of chemical potential in range  $0 \leq \mu_B \leq 450$  MeV and T between 30 MeV and 800 MeV. The equations respect the lattice QCD results up to  $l(\mu_B^4)$ . They consider existence of *cross-over transition*, *first order phase transition* and give possibility to choose the location of *Critical Point* on the QCD phase diagram  $\{T, \mu_B\}$ .

In the proposed EoS, the consistency with the derived from the first principle calculations is preserved. However, the problem with the limitation in the extraction of information about the medium characterized by the finite  $\mu_B$  is still present. Although the Taylor series used to expand the region studied with the QCD EoS never goes beyond the  $\mu_B$  higher than one at Critical Point, the universality class to which the Critical Point (CP) belongs is known, and it is possible to study the behaviour of EoS in some limited neighbourhood of CP.

The calculations applied by BEST are based on a strategy described in [3, 4]:

1. In the region close to CP, the suitable parametrization is used in the description of EoS universal scaling behaviour in the 3D Ising model;
2. The 3D Ising model phase diagram is mapped using a parametric change of variables (not universal)

onto the QCD one;

3. The Ising model thermodynamics is used to estimate the critical contribution to Lattice QCD expansion coefficients;
4. The full pressure is reconstructing - ensuring compatibility with Lattice QCD at  $\mu_B = 0$  and consisting the proper critical behaviour.

In the Fig. 1 the non-universal mapping procedure is illustrated. Using six parameters the critical thermodynamics is linearly transferred to QCD (Ising variables to QCD coordinates:  $(h, r) \mapsto (T, \mu_B)$ ).

Despite the possibility to locate the CP on the thermodynamics and hydrodynamic simulations, the proposed approach depends on the choice of parameters in the mapping of Ising  $\rightarrow$  QCD, which is not arbitrary. It is a consequence of a need to match Lattice QCD data which puts some limitations on the CP position.

### A. Selection of the EoS parameters

The primary studies possible due to the modifications and development of EPOS model allow one to study the impact on final observables of the changes between the variety of EoS. As mentioned in Section II, the BEST EoS is, in reality, the "family" of EoS, the set of various EoS tables. To obtain the EoS one needs to choose the set of parameters corresponding to mapping properties and locating the CP onto the QCD phase diagram.

The composition of the input parameters is crucial in setting the strength of the "criticality" of the transitions of the matter, moreover via changing the position of the CP one can expect the cross-over or the first-order transitions in the evolution of examined simulated systems. The structure of the parameter input file is:

```
MODE T0 κ μBC Δα1,α2 ω ρ
```

where:

- MODE - corresponds to the CP location and choice of following parameters. In this studies the CP lies on parabola parallel to the chiral transition line - what reports to  $MODE = PAR$ ;
- $T_0$  - the value of temperature at which the parabolic pseudo-critical line crosses the T axis;
- $\kappa$  - the curvature of the transition line at the T axis;
- $\mu_{BC}$  - the chemical potential at the critical point: since both critical temperature  $T_C$  and  $\alpha_1$  are determined by this choice, they do not need to be input;
- $\Delta_{\alpha_1, \alpha_2}$  - the difference between two angles (see Fig. 1)

- $\omega$  - the global scaling parameter in the mapping (the higher  $\omega$  the less criticality in transitions of matter);
- $\rho$  - the relative scaling in the mapping [4];

The  $T_C$ ,  $\alpha_{1,2}$  can be easily calculated from the given parameters:

$$T_C = T_0 + \kappa/T_0\mu_{BC}^2, \quad (1a)$$

$$\alpha_1 = 180/\pi \left| \arctan\left(-\frac{2\kappa}{T_0\mu_{BC}}\right) \right|, \quad (1b)$$

$$\alpha_2 = \alpha_1 + \Delta_{\alpha_1, \alpha_2} \quad (1c)$$

### III. EPOS MODEL

EPOS is an abbreviation of **E**nergy conserving quantum mechanical multiple scattering approach, based on **P**artons (parton ladders), **O**ff-shell remnants, and **S**aturation of parton ladders.

The model consists of several phases of evolution:

- initial stage (based on the Parton Gribov-Regge theory) [5, 6],
- core/corona division [7-9]
- hydrodynamical evolution [8],
- hadronization based on the given EoS,
- hadron rescattering (based on UrQMD [10, 11]),
- resonance decays.

In the model's theoretical framework, the crucial element is the sophisticated treatment of the hadron-hadron scattering and the initial stage of the collisions at ultra-relativistic energies. It is highly relevant in the understanding of possible parton-hadron phase transition. The merged approach of Gribov-Regge Theory (GRT) and the eikonalised parton model is utilised to provide proper treatment of the first interactions happening just after the collision - satisfying conservation laws and equal treatment of subsequent Pomerons [5, 6, 12].

If the density of the strings is very high, they cannot decay independently, and this situation is characteristic for the heavy-ions and the high-multiplicity  $p - p$  collisions. In EPOS the dynamical process of division of the strings segments into *core* and *corona* is introduced in order to deal with this issue [7-9].

The separation is based on the abilities of a given string segment to leave the "bulk matter". As the criteria for deciding, if it goes to a given group, the transverse momentum of the element and the local string density is taken into account. If the string segment belongs to the very dense area, it will not escape but will build the *core*, which will be driven in the next step by a hydrodynamical evolution. When the segment originates from the part of the string close to a kink, which is characterized

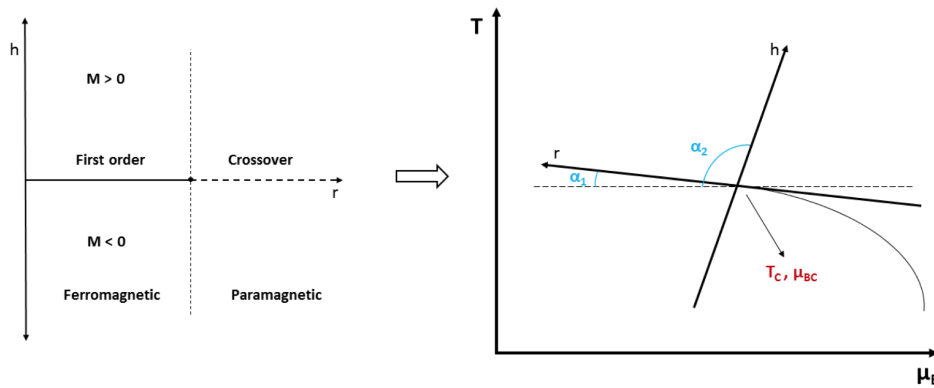


FIG. 1. The linear transformation is used in mapping the 3D Ising model diagram on the QCD one [4].

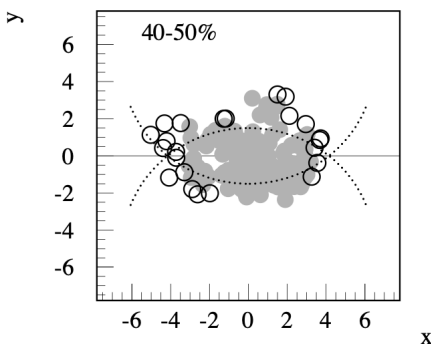


FIG. 2. The Monte Carlo simulation: full circles correspond to string segments contributing to core and open to corona. The big circles are just for the eye-guidance showing the surface of collided nuclei [9]

by the high transverse momenta, it escapes the bulk matter and join the *corona* and consequently will show up as a hadron (jet-hadrons). There is also a possibility that the string segment is close to the surface of the dense part of the medium, and its momentum is high enough to leave it; it also becomes a *corona* particle. The following equation is used for the determination of core and corona:

$$p_t^{new} = p_t - f_{Eloss} \int_{\gamma} \rho dL \quad (2)$$

where:  $\gamma$  is the trajectory of the segment,  $\rho$  the string density, and  $f_{Eloss}$  a non-zero constant for  $p_T > p_{T,1}$ , null for  $p_T < p_{T,2}$  and interpolated linearly between  $p_{T,1}$  and  $p_{T,2}$ . If the  $p_t^{new}$  is positive for a given segment, it escapes and becomes a corona particle; in the opposite case, it contributes to the core.

As it has been studied [13–16], the QGP does not expand like an ideal fluid, and the effect of the bulk viscosity has to be taken into account in the simulations. In EPOS, the 3D+1 viscous hydrodynamics is applied, providing an excellent description of the collective expansion of the matter [8].

In the simulations, the highly important is the definitive treatment of individual events - the generalization in considering smooth initial conditions for all events is not applied. The event-by-event (*ebe*) approach in hydrodynamical evolution is based on the random flux tube initial conditions [8]. It has a relevant impact on the final observables such as spectra or various harmonics of flow.

The final part of the simulation uses a so-called *hadronic afterburner* - UrQMD [10, 11].

When the density is very high and the mean free paths of constituent particles are small about any macroscopic length scale, the hydrodynamic description can be used - in the initial phase of the QGP evolution. With the cooling of the system, the density and the mean free paths decrease; oppositely, the  $\eta/s$  increases. Finally, the differences in the mean free path of various particle species become relevant, and the collective description of the system becomes not adequate. When the density and the temperature are low enough, the kinetic theory is applied using the UrQMD code [10, 11].

The particles can interact only when they leave the hyper-surface of the freeze-out. The  $2 \rightarrow n$  hadronic scattering is performed according to the measure reaction cross sections [17]. The 60 different baryonic species and their anti-particles, about 40 mesonic states are considered [10, 11]. There are implemented such interactions between hadrons as [18]:

- elastic scattering,
- string excitations,
- resonance excitations,
- strangeness exchange reactions

The hadronic scattering has a significant impact on the final observables [19, 20].

In this project, the possibility to introduce the new EoS was applied giving the possibility to study its impact on the simulation results.

## IV. RESULTS AND DISCUSSION

### A. Simulations

The two collision systems were studied: Au+Au collisions at  $\sqrt{s_{NN}} = 7.7$  GeV and 27 GeV (the lowest and the medium collision energy form Beam Energy Scan I at RHIC). The simulations using EPOS 3.4 model were performed using computer clusters at the Centre de Calcul de l'IN2P3/CNRS in Lyon. This is the preliminary version of the model, which is still under development. In the simulations the given Equations of State were applied:

- X3F cross-over, 3 flavour conservation [REF]
- BEST EoS with various parameters listed in Table I.

The only element of the whole simulation performed by EPOS model which changes is the Equation of State. Concluding, all the presented data sets can be used in the direct comparison of the proposed EoS. The "BEST 5" set of parameters was excluded due to the non-physical output.

### B. Production of particles

The production mechanism highly depends on the potentials characterising the system. The higher the  $\mu_B$ , the more produced baryons than antibaryons. Such relations are illustrated in Figure 3, where the most central 0 – 5% collisions of Au+Au simulated with EPOS 3.4 model are compared with STAR data published in [21]. Various EoS sets of parameters were used in performed simulations; the numbers of EPOS' data sets correspond to these listed in the Table I. The relations between particles' and antiparticles' production is reflected using ratios in Figure 4.

The higher number of produced baryons than antibaryons proves that in EPOS simulations, the impact of non-zero baryon potential is kept for all the proposed EoS. The model reflects the experimental data reasonably, except for pions. The number of these both negative and positive mesons is overestimated. Nonetheless, their ratio is kept.

The possible reason for such discrepancies could be the too wide rapidity distribution of simulated data. In the experimental analysis, the selection of particles characterised by the  $|y| < 0.1$  is very narrow. In such a case, even a small deviation in the rapidity distribution strongly affects the performed investigation.

In both Fig. 3 and 4 no relevant differences between simulations obtained with various EoS are observed. Notwithstanding the X3F Equation of State corresponds to the *cross-over* transition, which is not expected to happen for cooling systems created in collisions of Au+Au at  $\sqrt{s_{NN}} = 7.7$  GeV.

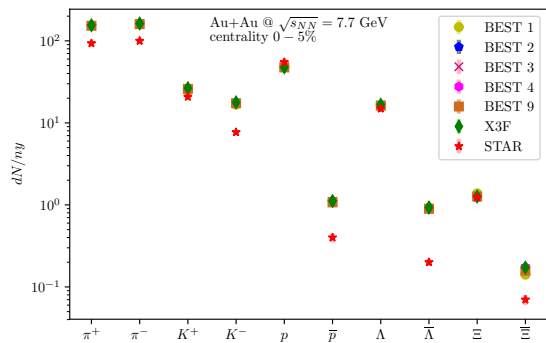


FIG. 3. Particle yields for Au+Au most central 0 – 5% collisions at  $\sqrt{s_{NN}} = 7.7$  GeV simulated with EPOS 3.4 model using various EoS and compared with STAR data [21].

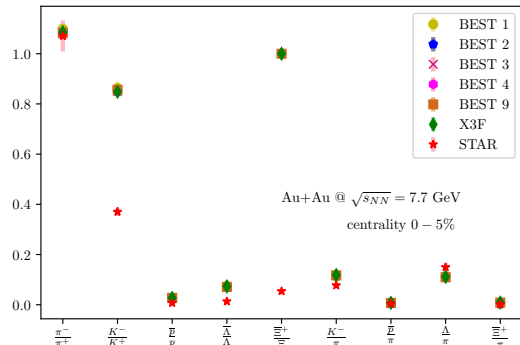


FIG. 4. Particle ratios for Au+Au most central 0 – 5% collisions at  $\sqrt{s_{NN}} = 7.7$  GeV simulated with EPOS 3.4 model using various EoS and compared with STAR data [21].

### C. Moments of particle distributions

The non-monotonic behaviour in the event-by-event fluctuations of globally conserved quantities is treated as one of the signatures of the presence of CP [22, 23]. The moments of distributions characterising the given fluctuations are:

- the mean ( $M$ )
- the standard deviation ( $\sigma$ )
- the skewness ( $S$ ), which corresponds to the asymmetry of the distribution
- the kurtosis ( $\kappa$ ), reflecting the degree to which the distribution is peaked relative to the normal distribution.

They are linked with the corresponding higher-order thermodynamic susceptibilities, and the system's correlation length [24, 25], which are expected to deviate for large samples in equilibrium at the CP. As a result of slowing down in the vicinity of CP, in reality, the system is driven away from the thermodynamic equilibrium, and the maximum value of correlation length attains 1.5-3 fm

TABLE I. Sets of input parameters for the construction of nine BEST EoS used in the EPOS simulations.

Number	MODE	$T_0$	$\kappa$	$\mu_{BC}$	$\Delta_{\alpha_{1,2}}$	$\omega$	$\rho$	$T_C$	$\mu_{BC}$	$\alpha_1$	$\alpha_2$	$\omega T_C$	$\rho \omega T_C$
BEST 1:	PAR	155	-0.0149	350	90	1	2	143	350	3	93	143	286
BEST 2:	PAR	155	-0.0149	350	90	4	1	143	350	3	93	572	572
BEST 3:	PAR	155	-0.0149	420	90	0.75	2	138	420	4	94	103	207
BEST 4:	PAR	155	-0.0149	350	90	10	1	143	350	3	93	1432	1432
BEST 5:	PAR	169	-0.0149	420	90	0.25	2	165	3	86	179	23599	6749k
BEST 6:	PAR	169	-0.0149	420	90	1	1	153	420	4	94	153	153
BEST 7:	PAR	169	-0.0149	420	90	0.5	1	153	420	4	94	76	76
BEST 8:	PAR	174	-0.0149	440	90	1	1	157	440	4	94	157	157
BEST 9:	PAR	178	-0.0149	300	90	1	1	170	300	2	92	170	170

[25]. During the fireball evolution after the hadronisation stage, the freeze-out signal information can dissipate [26]. However, if it survives, the higher moments can become useful in studies of CP's location. As the CP's location is changed in various used EoS, the moments of particle distributions are expected to be a useful tool in the performed investigation. In Figures 5 and 6 the comparison between two examined collision energies  $\sqrt{s_{NN}} = 7.7$  and 27 GeV are shown for  $S\sigma$  and  $\kappa\sigma^2$  as a function of number of participants. These combinations of moments are related directly with second and fourth order cumulants [27], which carry the information about possible critical behaviour of the system. Only BEST9 data set does not show the energy dependence, where the lower energy correspond to the higher values of  $S\sigma$ , what is the expected trend [28]. The significant disparities are present for various EoS for the  $\sqrt{s_{NN}} = 7.7$  GeV data even with the presence of high statistic uncertainties. Both  $S\sigma$  and  $\kappa\sigma^2$  for the  $\sqrt{s_{NN}} = 27$  does not show any multiplicity dependence.

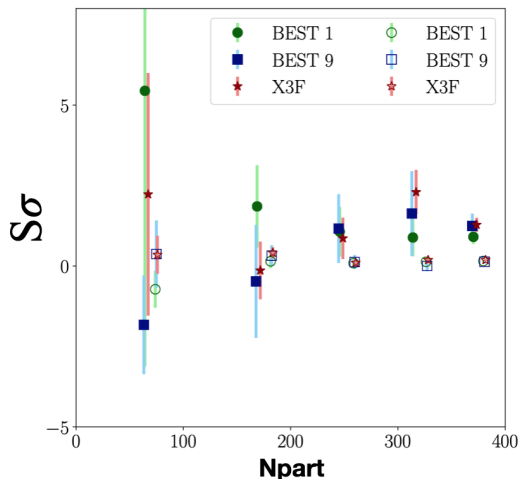


FIG. 5. The  $S\sigma$  for Au+Au collisions at  $\sqrt{s_{NN}} = 7.7$  (full markers) and 27 GeV (empty markers) as a function of number of participants. The shifts of the point on x-axis are applied for better visualisation.

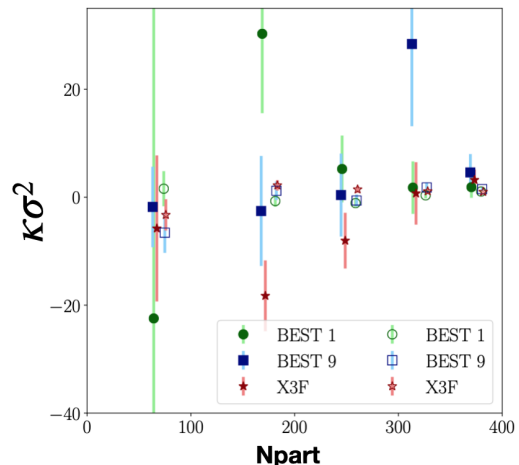


FIG. 6. The  $\kappa\sigma^2$  for Au+Au collisions at  $\sqrt{s_{NN}} = 7.7$  (full markers) and 27 GeV (empty markers) as a function of number of participants. The shifts of the point on x-axis are applied for better visualisation.

Figures 7 and 8 show the  $S\sigma$  and  $\kappa\sigma^2$  integrated overall centralities as a function of the collision energy. The significant energy dependence is present for  $S\sigma$  for all EoS. All the points at given energy are within the statistic errors, so no clear statement about the discrepancies between the EoS can be made.  $\kappa\sigma^2$  shows bigger variations between different EoS data sets. At  $\sqrt{s_{NN}} = 7.7$  GeV the highest point corresponds to the EoS where the CP is located at high  $T$  and low  $\mu_B$  and the simulated system is expected to go through the first-order transition, while the negative value is related with BEST 4, where the criticality is the less pronounced. For data sets simulated at  $\sqrt{s_{NN}} = 27$  GeV the differences are smaller; however, the BEST9 value is the highest. The energy dependence is not definite.

The measurements of the net-proton distributions' moments show the differences between data simulated using various Equations of State. They are more pronounced in peripheral collisions where we do not expect the big contribution from the "core" particles, so consequently less dependent on the EoS.

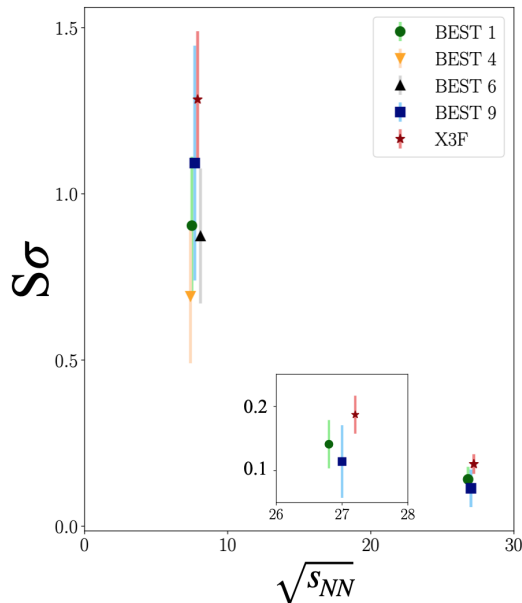


FIG. 7. The  $S\sigma$  for Au+Au collisions at  $\sqrt{s_{NN}} = 7.7$  and 27 GeV as a function of the collision energy  $\sqrt{s_{NN}}$ . The zoomed window corresponds to the points got collisions at  $\sqrt{s_{NN}} = 27$  GeV. The shifts of the point on x-axis are applied for better visualisation.

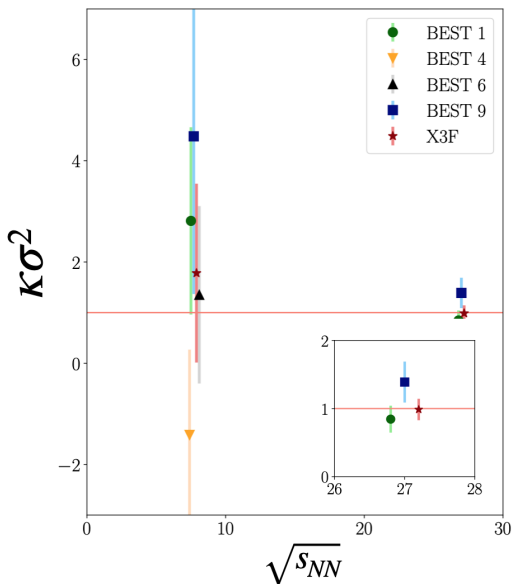


FIG. 8. The  $\kappa\sigma^2$  for Au+Au collisions at  $\sqrt{s_{NN}} = 7.7$  and 27 GeV as a function of the collision energy  $\sqrt{s_{NN}}$ . The zoomed window corresponds to the points got collisions at  $\sqrt{s_{NN}} = 27$  GeV. The shifts of the point on x-axis are applied for better visualisation.

## D. Particles' dynamics

The differences between the EoS were searched in the dynamics of the expanding matter. The listed below observables were investigated:

- transverse momentum spectra of identified hadrons: p,  $\bar{p}$ ,  $K^\pm$ ,  $\pi^\pm$  (Au+Au at  $\sqrt{s_{NN}} = 7.7$  and 27 GeV, 0 – 5% and 60 – 80% centrality ranges),
- elliptic flow of identified hadrons: p,  $\bar{p}$ ,  $K^\pm$ ,  $\pi^\pm$  (Au+Au at  $\sqrt{s_{NN}} = 7.7$  and 27 GeV, 0 – 80% centrality),
- event-by-event  $v_2^{obs}$ , not corrected with resolution of event plane (Au+Au at  $\sqrt{s_{NN}} = 7.7$  GeV, 0 – 80% centrality).

None of studied observables related to the expansion of the matter showed the variations between different EoS.

## V. CONCLUSION

The studies of various Equations of State implemented in the EPOS model were described. The development of the generator's code by introducing new EoS gave a unique possibility to investigate the impact of EoS on the final observables. Apart of the EoS, the whole structure of the model remained unchanged. The moments of net protons distributions gave important information about the variations of EoS. It makes the investigation of fluctuation of the particle distributions the most adequate observable for studies of the EoS.

## VI. ACKNOWLEDGMENTS

I would like to express the gratitude to Yurii Karpenko and Gabriel Sophys for fruitful discussions. This work was supported by the Grant of National Science Centre, Poland, No: 2021/41/B/ST2/02409 and 2020/38/E/ST2/00019. Studies were funded by IDUB-POB-FWEiTE-3, project granted by Warsaw University of Technology under the program Excellence Initiative: Research University (ID-UB), Deutsche Akademische Austauschdienst, and GET INVolved Programme.

[1] J. Adamczewski-Musch *et al.* (HADES), Probing dense baryon-rich matter with virtual photons, *Nature Phys.*

- [2] M. Stephanov, QCD phase diagram: An Overview, PoS **LAT2006**, 024 (2006), arXiv:hep-lat/0701002.
- [3] P. Parotto, Equation of state for QCD with a critical point from the 3D Ising Model, Nucl. Phys. A **982**, 183 (2019), arXiv:1808.03695 [hep-ph].
- [4] P. Parotto, Parametrized Equation of State for QCD from 3D Ising Model, *Proceedings, 11th International Workshop on Critical Point and Onset of Deconfinement (CPOD2017): Stony Brook, NY, USA, August 7-11, 2017*, PoS **CPOD2017**, 036 (2018), arXiv:1801.07801 [hep-ph].
- [5] V. Gribov, A REGGEON DIAGRAM TECHNIQUE, Sov. Phys. JETP **26**, 414 (1968).
- [6] H. J. Drescher, M. Hladik, S. Ostapchenko, T. Pierog, and K. Werner, Parton based Gribov-Regge theory, Phys. Rept. **350**, 93 (2001), arXiv:hep-ph/0007198 [hep-ph].
- [7] K. Werner, B. Guiot, I. Karpenko, and T. Pierog, Analysing radial flow features in p-Pb and p-p collisions at several TeV by studying identified particle production in EPOS3, Phys. Rev. **C89**, 064903 (2014), arXiv:1312.1233 [nucl-th].
- [8] K. Werner, I. Karpenko, T. Pierog, M. Bleicher, and K. Mikhailov, Event-by-Event Simulation of the Three-Dimensional Hydrodynamic Evolution from Flux Tube Initial Conditions in Ultrarelativistic Heavy Ion Collisions, Phys. Rev. **C82**, 044904 (2010), arXiv:1004.0805 [nucl-th].
- [9] K. Werner, Core-corona separation in ultra-relativistic heavy ion collisions, Phys. Rev. Lett. **98**, 152301 (2007), arXiv:0704.1270 [nucl-th].
- [10] M. Bleicher *et al.*, Relativistic hadron hadron collisions in the ultrarelativistic quantum molecular dynamics model, J. Phys. **G25**, 1859 (1999), arXiv:hep-ph/9909407 [hep-ph].
- [11] S. A. Bass *et al.*, Microscopic models for ultrarelativistic heavy ion collisions, Prog. Part. Nucl. Phys. **41**, 255 (1998), [Prog. Part. Nucl. Phys.41,225(1998)], arXiv:nucl-th/9803035 [nucl-th].
- [12] K. Werner, Strings, pomerons and the venus model of hadronic interactions at ultrarelativistic energies, Physics Reports **232**, 87 (1993).
- [13] N. Demir and S. A. Bass, Shear-viscosity to entropy-density ratio of a relativistic hadron gas, Phys. Rev. Lett. **102**, 172302 (2009).
- [14] A. El, A. Muronga, Z. Xu, and C. Greiner, Shear viscosity and out of equilibrium dynamics, Phys. Rev. **C 79**, 044914 (2009).
- [15] R. Snellings, Elliptic Flow: A Brief Review, New J. Phys. **13**, 055008 (2011), arXiv:1102.3010 [nucl-ex].
- [16] C. Gale, S. Jeon, and B. Schenke, Hydrodynamic Modeling of Heavy-Ion Collisions, Int. J. Mod. Phys. **A28**, 1340011 (2013), arXiv:1301.5893 [nucl-th].
- [17] C. Patrignani *et al.* (Particle Data Group), Review of Particle Physics, Chin. Phys. C **40**, 100001 (2016).
- [18] J. Steinheimer, V. Vovchenko, J. Aichelin, M. Bleicher, and H. Stöcker, Final state hadronic rescattering with UrQMD, EPJ Web Conf. **171**, 05003 (2018).
- [19] M. Stefaniak, Examination of Heavy-ion Collisions Using EPOS Model in the Frame of BES Program, *Proceedings, NICA days 2017: Warsaw, Poland, November 6-10, 2017*, Acta Phys. Polon. Supp. **11**, 695 (2018).
- [20] J. Steinheimer, V. Vovchenko, J. Aichelin, M. Bleicher, and H. Stöcker, Conserved charge fluctuations are not conserved during the hadronic phase, Phys. Lett. B **776**, 32 (2018), arXiv:1608.03737 [nucl-th].
- [21] L. Adamczyk *et al.* (STAR), Bulk Properties of the Medium Produced in Relativistic Heavy-Ion Collisions from the Beam Energy Scan Program, Phys. Rev. **C96**, 044904 (2017), arXiv:1701.07065 [nucl-ex].
- [22] S. Sombun, J. Steinheimer, C. Herold, A. Limphirat, Y. Yan, and M. Bleicher, Higher order net-proton number cumulants dependence on the centrality definition and other spurious effects, J. Phys. G **45**, 025101 (2018), arXiv:1709.00879 [nucl-th].
- [23] X. Luo and N. Xu, Search for the QCD Critical Point with Fluctuations of Conserved Quantities in Relativistic Heavy-Ion Collisions at RHIC : An Overview, Nucl. Sci. Tech. **28**, 112 (2017), arXiv:1701.02105 [nucl-ex].
- [24] M. Stephanov, Non-Gaussian fluctuations near the QCD critical point, Phys. Rev. Lett. **102**, 032301 (2009), arXiv:0809.3450 [hep-ph].
- [25] C. Athanasiou, K. Rajagopal, and M. Stephanov, Using Higher Moments of Fluctuations and their Ratios in the Search for the QCD Critical Point, Phys. Rev. D **82**, 074008 (2010), arXiv:1006.4636 [hep-ph].
- [26] M. Stephanov, Evolution of fluctuations near QCD critical point, Phys. Rev. D **81**, 054012 (2010), arXiv:0911.1772 [hep-ph].
- [27] D. Oliinychenko, S. Shi, and V. Koch, Effects of local event-by-event conservation laws in ultrarelativistic heavy-ion collisions at particlization, Phys. Rev. C **102**, 034904 (2020), arXiv:2001.08176 [hep-ph].
- [28] M. Aggarwal *et al.* (STAR), Higher Moments of Net-proton Multiplicity Distributions at RHIC, Phys. Rev. Lett. **105**, 022302 (2010), arXiv:1004.4959 [nucl-ex].